Available online at www.sciencedirect.com
ScienceDirect
Electrochemistry Communications 13 (2008) 455–460
electrochemistry communications
www.elsevier.com/locate/elecom

Combustion synthesized $LiMnSnO_4$ cathode for lithium batteries

N. Jayaprakash [a], N. Kalaiselvi [a,*], Y.K. Sun [b]

[a] Central Electrochemical Research Institute, Karaikudi, 630 006, India
[b] Department of Chemical Engineering, Center for Information and Communication Materials, Hanyang University, Seoul 133-791, South Korea

Received 26 November 2007; received in revised form 20 December 2007; accepted 21 December 2007

Abstract

Novel category $LiMnSnO_4$ compound was synthesized via. Urea assisted combustion (UAC) method at 800 °C and examined for possible use as cathode material in lithium-ion batteries. The XRD (X-ray diffraction) results of $LiMnSnO_4$ sample authenticate the orthorhombic crystal structure with high degree of crystallinity. Presence of uniformly distributed nanometric grains (scanning electron microscopy) with preferred local cation environment is evident from FT IR (Fourier transform infra red spectroscopic) and ^7Li NMR (nuclear magnetic resonance spectroscopy) studies. The charge–discharge behavior of $Li/LiMnSnO_4$ cells demonstrated a specific capacity of 113 mA h/g, with an excellent capacity retention (95%) and Ah efficiency (>99%). Besides, the internal resistance of the $Li/LiMnSnO_4$ cell after 30 cycles is negligibly small, thus demonstrating good electronic conductivity and cycling stability, required for any lithium intercalating cathode material.

Keywords: $LiMnSnO_4$ cathode; MAS ^7Li NMR; Orthorhombic; Urea assisted combustion method; Lithium-ion battery

1. Introduction

Compounds that can reversibly incorporate lithium ions into their crystal structures are of interest for application as cathode materials in rechargeable lithium batteries [1]. Common cathode materials used in lithium batteries are spinel $LiMn_2O_4$ [2], layered $LiCoO_2$ [3], $LiNiO_2$ [4] and the olivine category $LiFePO_4$ [5]. Basically, the deployment of $LiMn_2O_4$ cathode in practical devices is limited, as it suffers from poor capacity retention due to Jahn-Teller distortion induced metal dissolution [2]. On the other hand, the most commonly used $LiCoO_2$ and the high capacity $LiNiO_2$ cathodes need to be addressed for their toxicity, cost and safety issues [6]. Similarly, phospho-olivines, popularly known for their low cost, nontoxicity and high inherent safety also have low electronic conductivity and slow lithium ion diffusion across the $LiFePO_4/FePO_4$ boundary problems, thus necessitates the search for newer and alternate cathode materials for lithium battery applications.

Besides olivines, it is believed that there is ample hope for $LiMSnO_4$ category compounds as possible lithium insertion electrodes [1,7], wherein report on $LiFeSnO_4$ compound alone is available in the literature till date [8]. Based on the intriguing results of such a preliminary explorative study on $LiFeSnO_4$ compound [1,8], it was decided to synthesize a related category eco-benign and economically viable $LiMnSnO_4$ compound, so as to explore the possibility of deploying the same as cathode in rechargeable lithium cells. Hence, a detailed investigation on $LiMnSnO_4$ compound has been made for the first time with a view to understand the structural and electrochemical behavior of the same for exploitation as lithium intercalating cathode material.

As is well known that the synthesis procedure adopted plays a vital role in deciding the specific capacity and capacity fade of an electrode material, Urea assisted combustion (UAC) method has been chosen for the present work, based on our earlier studies [9]. As expected, UAC method has resulted in the formation of ultra fine LiM-

* Corresponding author. Tel.: +91 4565 227550x559; fax: +91 4565 227779.
E-mail address: kalakanth2@yahoo.com (N. Kalaiselvi).

1388-2481/$ - see front matter © 2007 Elsevier B.V. All rights reserved.
doi:10.1016/j.elecom.2007.12.029

$nSnO_4$ powders with desirable physical as well as electrochemical characteristics of lithium intercalating cathode material, which is the significance of present study.

2. Experimental

2.1. Synthesis procedure

The $LiMnSnO_4$ active material was synthesized by adopting Urea assisted combustion (UAC) method where stoichiometric proportions of respective high purity metal nitrate (Sigma Aldrich, India) precursors were dissolved in triple distilled water. To the homogeneous solution was added calculated quantity of urea, a popularly known combustion fuel, along with continuous stirring. The clear solution thus obtained after the addition of urea was heat treated at 120 °C for 12 h. followed by sintering at 300 °C for about 5 h. to expel carbon in the form of CO_2 that resulted from the combustion of urea. The sintered precursor obtained at this stage was ground to yield finer powder and was further heat treated at a higher temperature of 800 °C for 3 h. using an alumina crucible. Herein, both the rate of heating and cooling were maintained at 1 °C/min to avoid surface cracking of the particles and to ensure the presence of uniformly distributed particles of submicron size. Also, the properly controlled and duly monitored heating sequence renders improved yield (70%) of the final product without any undesirable agglomeration that takes place normally during high temperature sintering process.

2.2. Physical and electrochemical characterization

Phase characterization was done from the powder X-ray diffraction (XRD) patterns recorded on a Philips 1830 X- ray diffractometer using Ni filtered Cu Kα

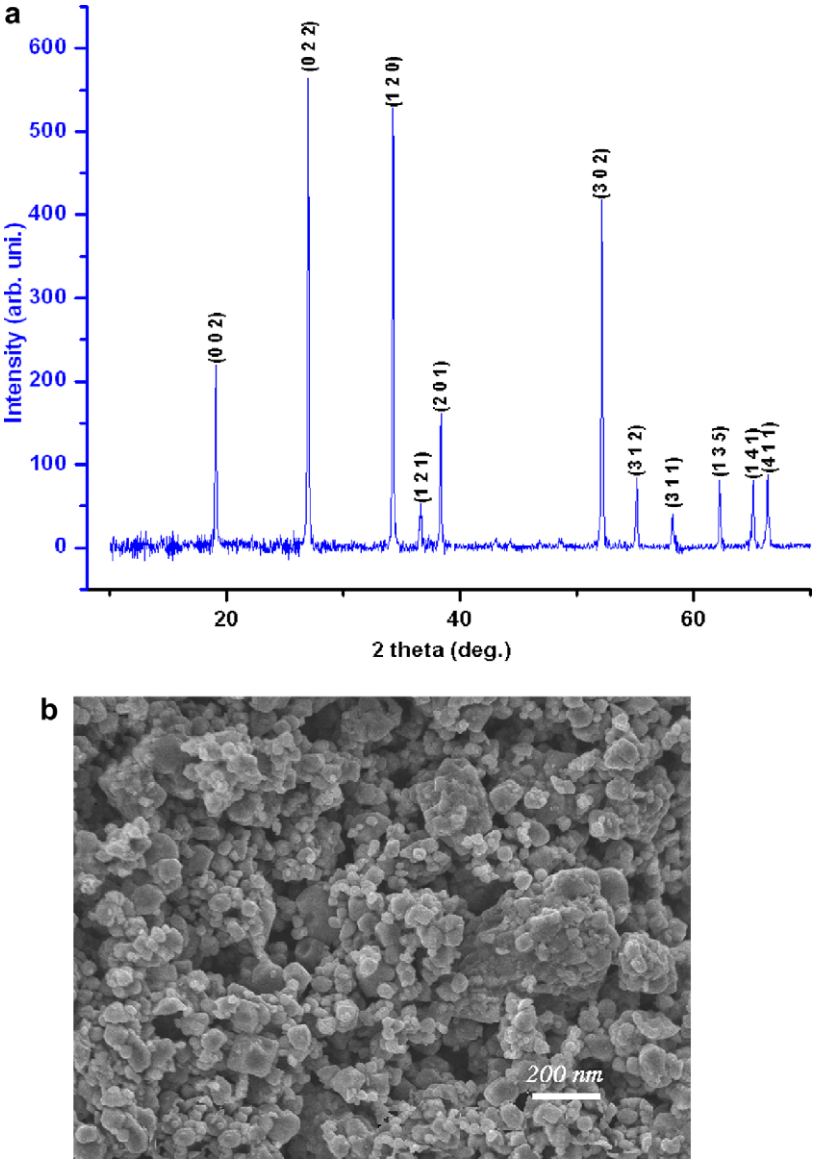

Fig. 1. (a) X-ray diffraction pattern and (b) SEM image of $LiMnSnO_4$ compound calcined at 800 °C.

radiation ($\lambda = 1.5406$ Å). Surface morphology of the synthesized $LiMnSnO_4$ was investigated using Jeol S-3000H Scanning Electron Microscope. Fourier transform infra red spectroscopy (FT IR) study was performed on a Perkin-Elmer paragon-500 FT IR spectrophotometer using a pellet containing the mixture of KBr and the active material in the region of 400–2000 cm^{-1}. ^7Li NMR measurements were carried out with a Bruker MSL-400 spectrometer by employing a 5 mm Bruker VT-MAS probe operating at a ^7Li frequency of 14 MHz. Electrochemical impedance spectroscopy (EIS) measurement and charge–discharge measurements were performed using an Autolab Electrochemical Workstation and MACCOR charge–discharge cycle life tester respectively.

2.3. Electrode preparation and cell assembly

The process of electrode preparation and the coin cell fabrication in an Argon-filled Glove box are mentioned in our earlier reports [10].

3. Results and discussion

3.1. Structural and surface morphology results

Fig. 1a shows the PXRD (Powder X-ray diffraction) pattern of $LiMnSnO_4$ material synthesized at 800 °C by UAC method. The existence of well defined and highly intense Bragg peaks demonstrates the presence of phase pure and highly crystallized product**.** The deployment of optimum synthesis temperature (800 °C) with an intermittent grinding has excluded the co-existence of undesirable impurities associated with the formation of $LiMnSnO_4$. The miller indices *(hkl)* of all the peaks corresponding to $LiMnSnO_4$ are indexed as per the JCPDS file No: 310767 that corroborates the existence of an orthorhombic lattice structure. The lattice parameter values calculated by least square fitting are $a = 5.30$, $b = 6.01$, and $c = 9.08$. Using Scherer's formula [11], the average grain size of $LiMnSnO_4$ has been calculated to be 250 nm, which is believed to be due to the deployment UAC method to produce ultra fine powders of $LiMnSnO_4$.

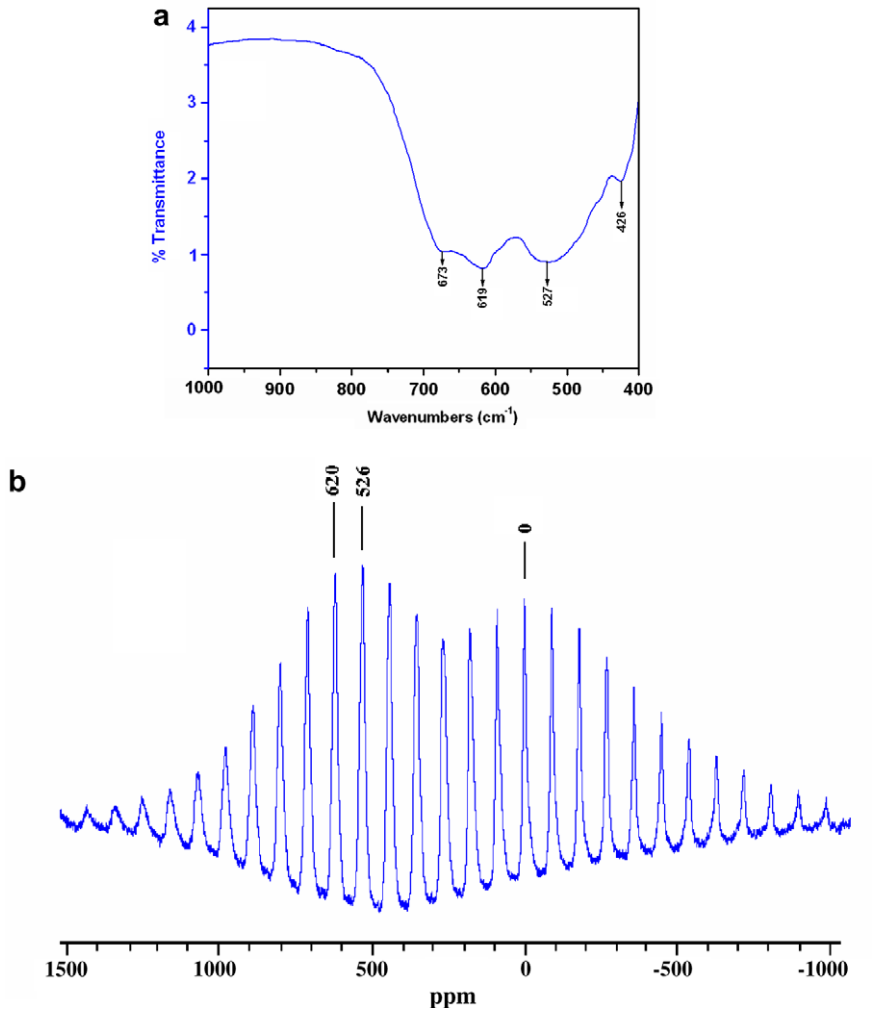

Fig. 2. (a) FT IR and (b) ^7Li MAS NMR spectra of $LiMnSnO_4$.

The surface morphology of $LiMnSnO_4$ compound has been investigated using Scanning electron microscopy (Fig. 1b). Presence of evenly distributed spherical grains with well defined grain boundary and particles in the order of ~200 nm is obvious from the micrographs of $LiMnSnO_4$. Thus the presence of nanometric grain size of $LiMnSnO_4$, as derived from Scherer's formula is substantiated further from SEM studies.

3.2. FT IR and MAS ^{7}Li NMR studies

FT IR signature of $LiMnSnO_4$ (Fig. 2a) compound consists of high frequency bands at 619 and 527 cm^{-1}, due to the asymmetric stretching modes of the MnO_6 group [12]. Similarly, a weak band at 426 cm^{-1} is assigned to the vibrations of LiO_4 tetrahedra [12] and the presence of a new and an additional weak band at 673 cm^{-1} may be attributed to the presence of edge sharing SnO_6 octahedra.

The broad room temperature ^{7}Li NMR spectra recorded for $LiMnSnO_4$ compound (Fig. 2b) consists of two intense resonances at 620 and 526 ppm and a less intense resonance at 0 ppm. It is quite interesting to note that the ^{7}Li NMR results of our earlier study conducted on a series of $LiMSnO_4$ with M = Ni, Al, Ce and Co have demonstrated the presence of single resonance at 0 ppm alone, suggesting the presence of orthorhombic type of

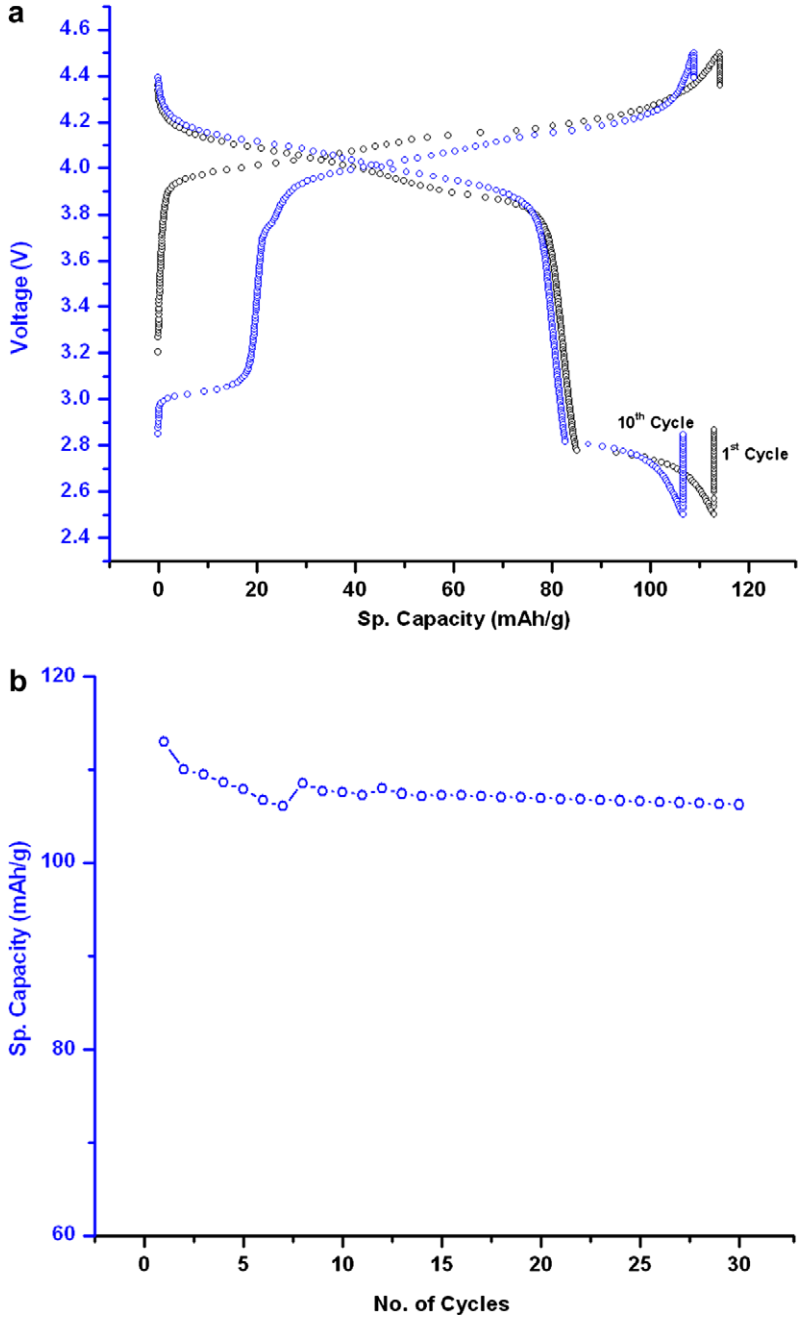

Fig. 3. (a) Voltage *vs.* Sp. Capacity and (b) Sp. Capacity *vs.* Cycle number behavior of $LiMnSnO_4$.

arrangement [13]. On the contrary, when Mn is substituted for M in $LiMSnO_4$ matrix, it is evident from present study, that the Li site occupancy experiences a major shift towards high frequency region (620–520 ppm), in addition to the normal 0 ppm resonance, which is unusual. However, the presence of additional resonances at 526 and 620 ppm in the present study may be corroborated with the manganese induced defect mechanism that leads to the partial occupation of Li in 8a tetrahedral sites and the presence of lithium near 16d manganese vacancies respectively [14].

3.3. Electrochemical characterization-charge discharge studies

The electrochemical performance characteristics of $LiMnSnO_4$ cathode measured on a coin cell at a constant current density of 0.2 mA and in the potential window of 2.8–4.5 V demonstrate the reversibility and structural stability of the same upon cycling.

Fig. 3a shows the charge–discharge behavior of Li/$LiMnSnO_4$ half-cell, wherein the compound exhibited two voltage plateaus around 3.9 and 4.1 V that may be attributed to the insertion and extraction of lithium ions in two stages [15]. As seen from Fig. 3a, the compound exhibited similar charge (114 mA h/g) and discharge capacity (113 mA h/g) values, thus demonstrating the excellent columbic efficiency (>99%). Further, the exact overlapping of the initial discharge (Qd_{c1}) curve with the one obtained after 10 cycles (Qd_{c10}) demonstrates the excellent capacity retention and structural stability of the $LiMnSnO_4$ cathode, especially upon cycling.

Fig. 3b represents the cycle life *vs.* capacity plot of $LiMnSnO_4$ cathode examined at room temperature, wherein an initial discharge capacity of 113 mA h/g with a reversible capacity of 108 mA h/g at the end of 30 cycles has been displayed by the compound. Such a high degree of capacity retention (>95%) exhibited by $LiMnSnO_4$ may be correlated to the combined effect of enhanced conductivity and structural stability of the cathode. The average capacity loss in $LiMnSnO_4$ cathode per cycle (~0.17%) is almost negligible, thus qualifying the same as a potential cathode with near zero strain electrode behavior.

The high stability of the $LiMnSnO_4$ cathode upon cycling was further confirmed from the electrochemical impedance analysis carried out for both the as fabricated and the cell after completing 30 cycles (Fig. 4). It is evident from Fig. 4 that the high frequency region intercept values with the real impedance [Re(Z)] are 51 and 54 Ω respectively, corresponding to the total electrical resistance of the as fabricated $LiMnSnO_4$ cell and the cell after 30 cycles. It is well known that such an intercept value is considered as the total electrical resistance offered by the electrode material (R_m), electrolyte (R_e), and the electrical leads [16]. Since the resistance of electrolyte (R_e) and that of electrical leads (R_l) are almost the same throughout the experiments, the small difference in the total resistance of $LiMnSnO_4$ cathode corresponds to the resistance of the synthesized cathode. Hence, it is understood from EIS measurements also that the synthesized $LiMnSnO_4$ cathode possesses good electrochemical stability upon extended cycling, as the internal resistance of the cell after cycling has not increased significantly.

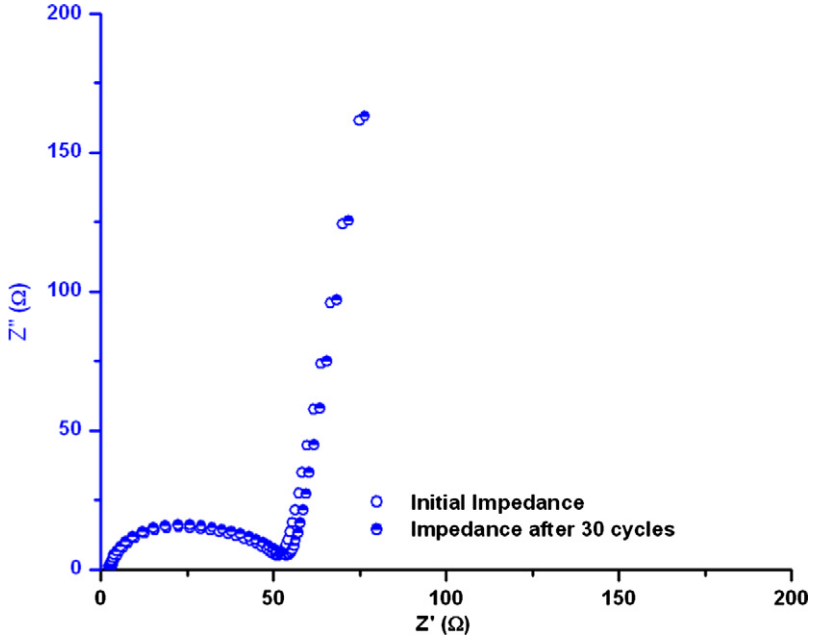

Fig. 4. Nyquist impedance spectra of $LiMnSnO_4$.

4. Conclusion

In an attempt to explore the novel category $LiMnSnO_4$ cathode for rechargeable lithium batteries, Urea assisted combustion (UAC) method has been chosen to synthesize the title compound. Nanometric $LiMnSnO_4$ powders with high phase purity and crystallinity were obtained at 800 °C. Presence of orthorhombic crystal structure is evident from XRD and ^7Li NMR, despite the presence of additional resonance due to the manganese induced defect in $LiMnSnO_4$ matrix. An apparently high specific capacity of ~113 mA h/g has been exhibited by the UAC synthesized $LiMnSnO_4$ cathode with good electrochemical stability upon extended cycling. The appreciable electrochemical characteristics, especially the excellent columbic efficiency (>99%) and better capacity retention upon cycling (~0.17% capacity fade) qualify the $LiMnSnO_4$ cathode as one of the promising next generation strain free electrodes for use in lithium batteries.

Acknowledgements

The authors are thankful to the Department of Science and Technology (DST), New Delhi for financial support to carry out this work. Also, the authors thank Shri. S. Radhakrishnan for recording ^7Li NMR data.

References

[1] M. Greenblat, E. Wang, H. Eckert, N. Kimura, R.H. Herber, J.V. Waszczak, Inorg. Chem. 24 (1985) 1661.
[2] J.C. Arrebola, A. Caballero, M. Cruz, L. Hernán, J. Morales, E.R. Castellón, Adv. Funct. Mater. 16 (2006) 1904.
[3] Q. Cao, H.P. Zhang, G.J. Wang, Q. Xia, Y.P. Wu, H.Q. Wu, Electrochem. Commun. 9 (2007) 1228.
[4] J. Kim, K. Amine, Electrochem. Commun. 3 (2001) 52.
[5] A.K. Padhi, K.S. Nanjundaswamy, J.B. Goodenough, J. Electrochem. Soc. 144 (1997) 1188.
[6] Y.J. Lee, F. Wang, C.P. Grey, J. Am. Chem. Soc. 120 (1998) 12601.
[7] M.V.V.M. Satya Kishore, U.V. Varadaraju, B. Raveau, J. Solid State Chem. 177 (2004) 3981.
[8] J. Choisnet, M. Hervieu, B. Raveau, P. Tarte, J. Solid State Chem. 40 (1981) 344.
[9] R. Kalai Selvan, N. Kalaiselvi, C.O. Augustin, C.H. Doh, Electrochem. Solid-State Lett. 9 (8) (2006) A390.
[10] N. Kalaiselvi, C.-H. Doh, C.-W. Park, S.-I. Moon, M.-S. Yun, Electrochem. Commun. 6 (2004) 1110.
[11] N. Jayaprakash, N. Kalaiselvi, Electrochem. Commun. 9 (2007) 620.
[12] P. Kalyani, N. Kalaiselvi, N. Muniyandi, J. Power Sources 111 (2002) 232.
[13] N. Jayaprakash, N. Kalaiselvi, J. Phys.: Cond. Matter, submitted for publication.
[14] Y.J. Lee, F. Wang, C.P. Grey, J. Am. Chem. Soc. 120 (1998) 2601.
[15] B.L. He, W.J. Zhou, Y.Y. Liang, S.J. Bao, H.L. Li, J. Colloid Interf. Sci. 300 (2006) 633.
[16] C.Y. Lee, H.M. Tsai, H.J. Chuang, S.Y. Li, P. Lin, T.Y. Tseng, J. Electrochem. Soc. 152 (4) (2005) A716.